

Facile synthesis of highly SERS active nanosilver sol with microwave and its application to detect *E. coli* using Vicrtoia blue B as molecular probe

Yaohui Wang, Xinghui Zhang, Guiqing Wen, Aihui Liang* and Zhiliang Jiang*

Key Laboratory of Ecology of Rare and Endangered Species and Environmental Protection of Ministry Education, Guangxi
Normal University, Guilin 541004, China

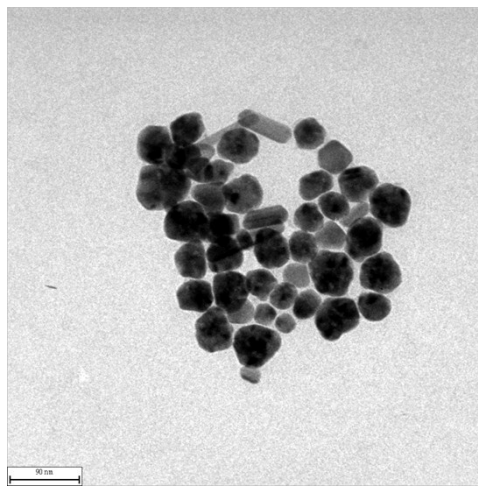


Fig. S1 TEM of the AgNPs using diethanolamine as a reductant

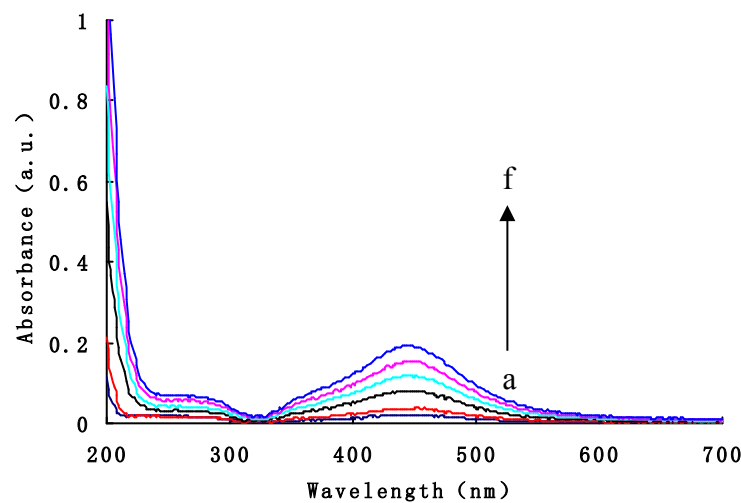


Fig. S2 SPR absorption spectra of the AgNRs

(a) 0.5 μg/ml AgNPs; (b) 1 μg/ml AgNPs; (c) 2 μg/ml AgNPs; (d) 3 μg/ml AgNPs; (e) 4 μg/ml AgNPs; (f) 5 μg/ml AgNPs

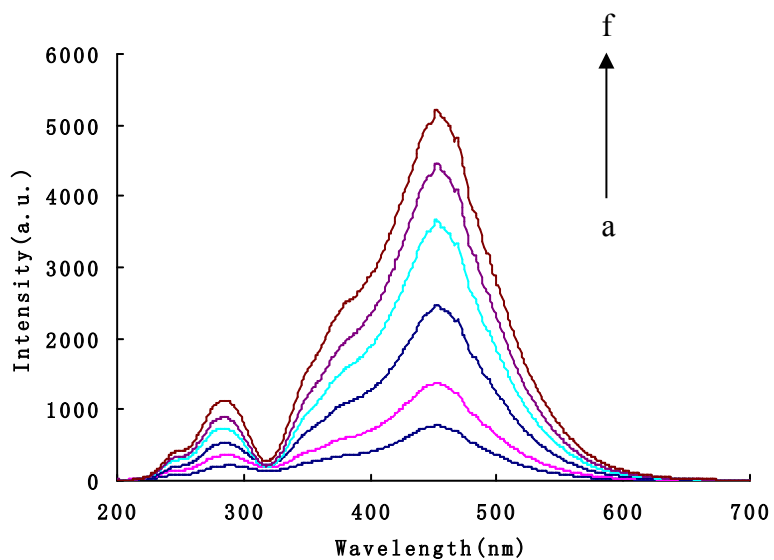


Fig. S3 RRS spectra of AgNRs

(a) 0.5 $\mu\text{g}/\text{ml}$ AgNPs; (b) 1 $\mu\text{g}/\text{ml}$ AgNPs; (c) 2 $\mu\text{g}/\text{ml}$ AgNPs; (d) 3 $\mu\text{g}/\text{ml}$ AgNPs; (e) 4 $\mu\text{g}/\text{ml}$ AgNPs; (f) 5 $\mu\text{g}/\text{ml}$ AgNPs

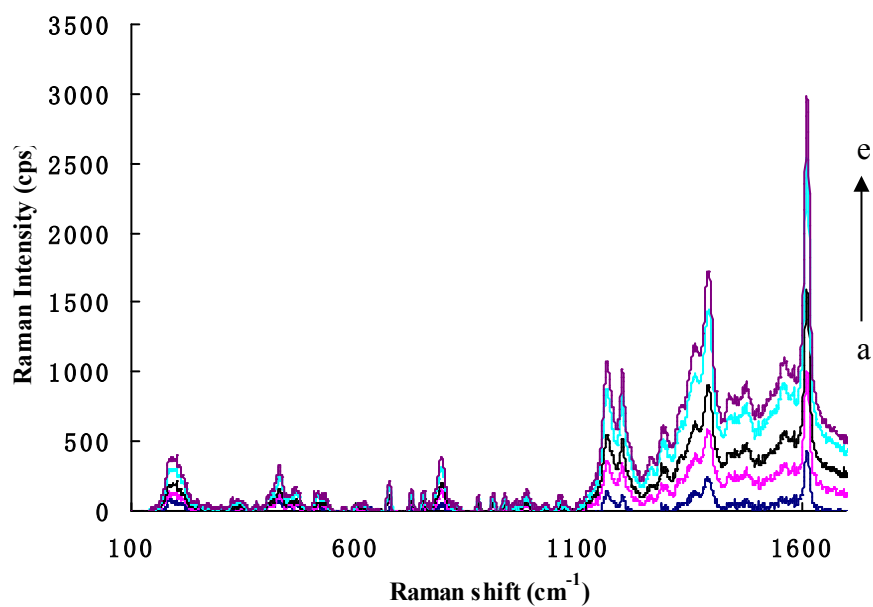


Fig S4 SERS spectra of AgNPs

(a) 2 $\mu\text{g}/\text{mL}$ AgNPs+0.25 $\mu\text{mol}/\text{L}$ VBB +pH 6.8 PBS+1.5 mmol/L NaCl; (b) 3 $\mu\text{g}/\text{mL}$ AgNPs+0.25 $\mu\text{mol}/\text{L}$ VBB +0.25 mol/L NaCl;
 (c) 4 $\mu\text{g}/\text{mL}$ AgNPs+0.25 $\mu\text{mol}/\text{L}$ VBB +0.25 mol/L NaCl; (d) 5 $\mu\text{g}/\text{mL}$ AgNPs+0.25 $\mu\text{mol}/\text{L}$ VBB +0.25 mol/L NaCl; (e) 6 $\mu\text{g}/\text{mL}$
 AgNPs+0.25 $\mu\text{mol}/\text{L}$ VBB +0.25 mol/L NaCl.

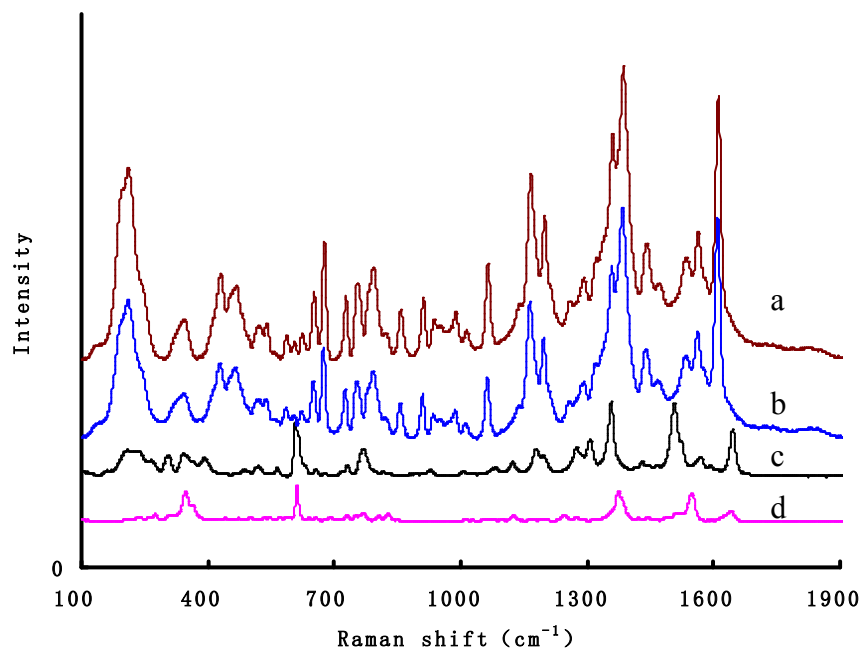


Fig. S5 SERS spectra of VBB, VB4R, AR and ST stained *E. coli*. a: 5 µg/mL AgNPs-1.5×10⁻³ mol/L NaCl-0.01 µg/mL AgNO₃-pH 6.8 PBS-5.0×10⁸ cfu/ml VBB-*E. coli*; b: 5 µg/mL AgNPs-1.5×10⁻³ mol/L NaCl-pH 6.8 PBS-5.0×10⁸ cfu/ml VB4R-*E. coli*; c: 5 µg/mL AgNPs-1.5×10⁻³ mol/L NaCl-pH 6.8 PBS-5.0×10⁸ cfu/ml AR-*E. coli*; d: 5 µg/mL AgNPs-1.5×10⁻³ mol/L NaCl-pH 6.8 PBS-5.0×10⁸ cfu/ml ST-*E. coli*.

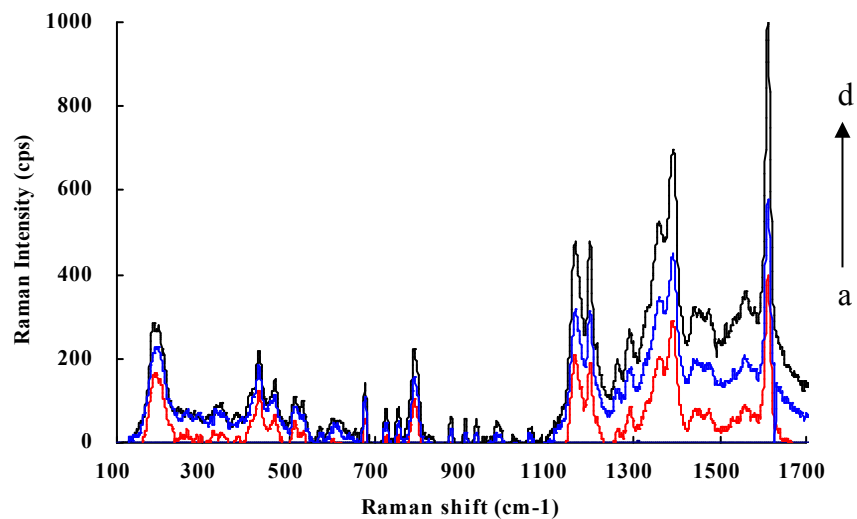


Fig S6 SERS spectra of VBB-*B. subtilis*

a: 5 µg/mL AgNPs-2 µmol/L AgNO₃-1.5×10⁻³ mol/L NaCl-0.01 µg/mL AgNO₃-pH 6.8 PBS; b: a-1.25×10⁸/mL *B. subtilis*; c: a-2.5×10⁸/mL *B. subtilis*; d: a-3.75×10⁸/mL *B. subtilis*.

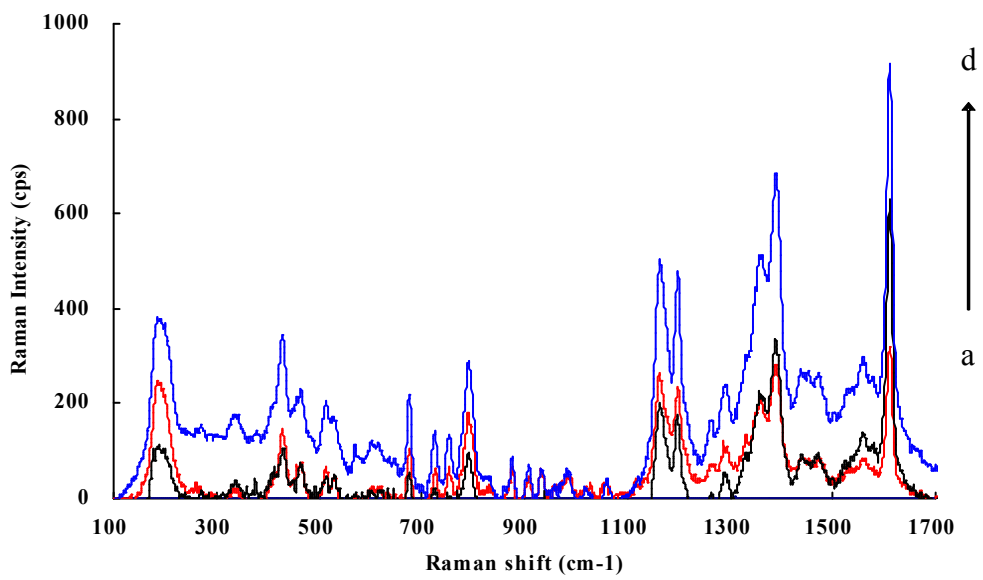


Fig. S7 SERS spectra of VBB-*S. aureus*

a: 5 $\mu\text{g}/\text{mL}$ AgNPs -2 $\mu\text{mol}/\text{L}$ AgNO₃-1.5×10⁻³ mol/L NaCl-0.01 $\mu\text{g}/\text{mL}$ AgNO₃-pH 6.8 PBS; b: a-4.8×10⁴/mL *S. aureus*; c: a-9.6×10⁴/mL *S. aureus*; d: a-14.4×10⁴/mL *S. aureus*.

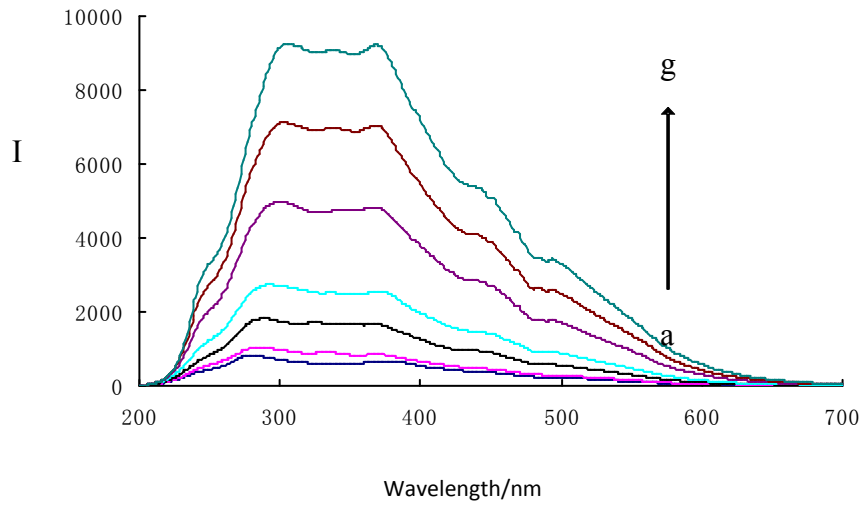


Fig. S8 RRS spectra of *B. subtilis*

a: 1×10⁸/mL *B. subtilis*; b: 2×10⁸/mL *B. subtilis*; c: 4×10⁸/mL *B. subtilis*; d: 8×10⁸/mL *B. subtilis*; e: 16×10⁸/mL *B. subtilis*; f: 24×10⁸/mL *B. subtilis*; g: 32×10⁸/mL *B. subtilis*.

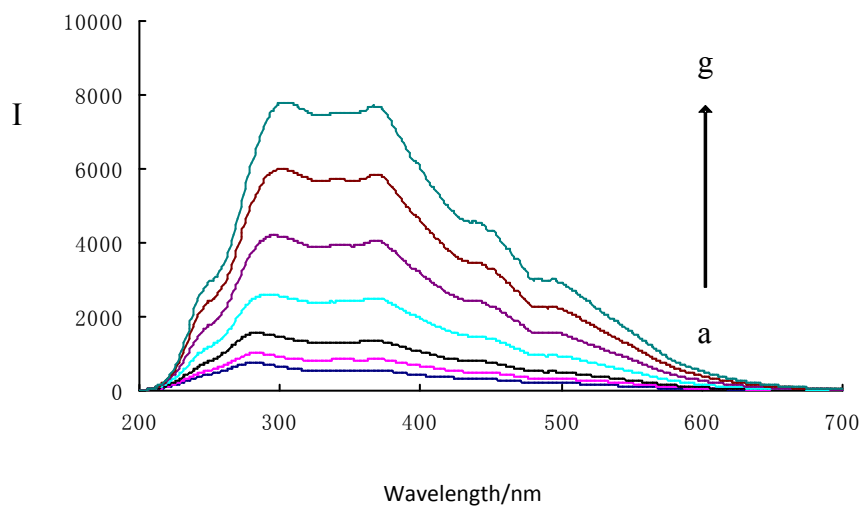


Fig. S9 RRS spectra of *S. aureus*

a: 0.65×10^5 /mL *S. aureus*; b: 1.3×10^5 /mL *S. aureus*; c: 2.6×10^5 /mL *S. aureus*; d: 5.2×10^5 /mL *S. aureus*; e: 10.4×10^5 /mL *S. aureus*; f: 15.6×10^5 /mL *S. aureus*; g: 20.8×10^5 /mL *S. aureus*.

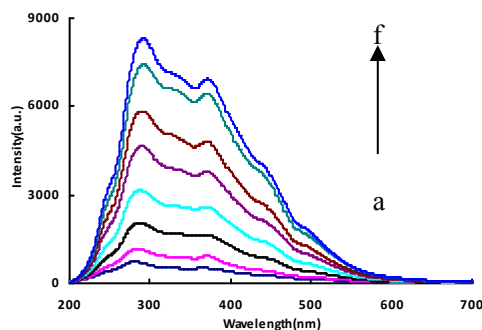


Fig. S10 RRS spectra of VBB- *E. coli*. a: 1.5×10^8 cfu/mL VBB-*E. coli*; b: 3.0×10^8 cfu/mL VBB-*E. coli*; c: 6.0×10^8 cfu/mL VBB-*E. coli*; d: 12×10^8 cfu/mL VBB-*E. coli*; e: 24×10^8 cfu/mL VBB-*E. coli*; f: 36×10^8 cfu/mL VBB-*E. coli*.

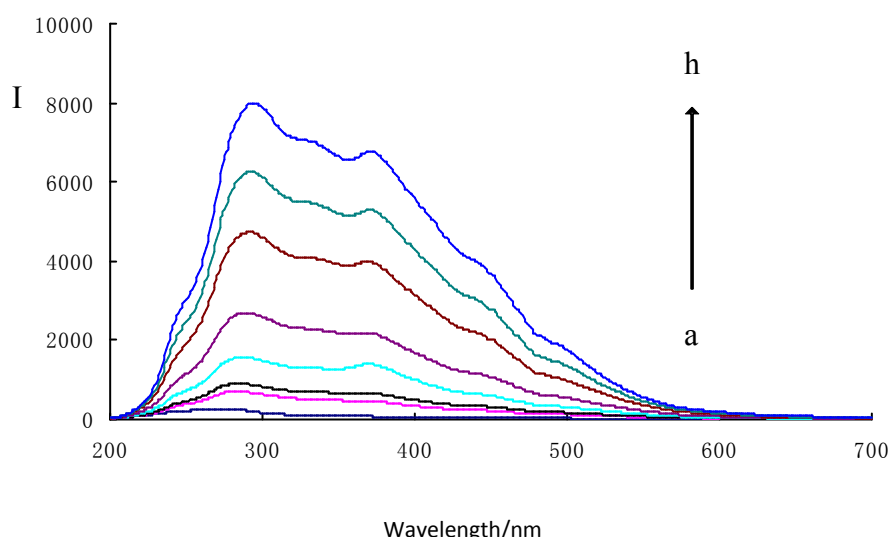


Fig. S11 RRS spectra of VBB- *B. subtilis*

a:water; b: 1.25×10^8 /mL VBB-*B. subtilis*; c: 2.5×10^8 /mL VBB-*B. subtilis*; d: 5×10^8 /mL VBB-*B. subtilis*; e: 10×10^8 /mL VBB-*B. subtilis*; f: 20×10^8 /mL VBB-*B. subtilis*; g: 30×10^8 /mL VBB-*B. subtilis*; h: 40×10^8 /mL VBB-*B. subtilis*.

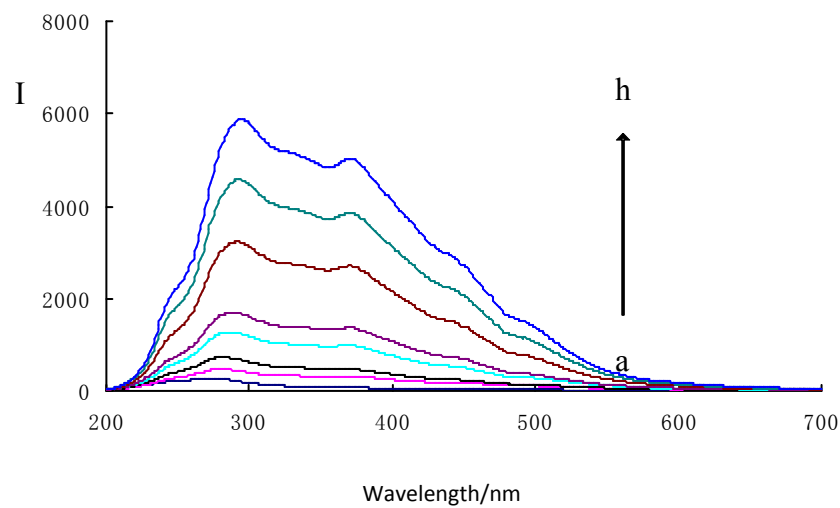


Fig. S12 RRS spectra of VBB- *S. aureus*

a: water; b: 0.32×10^5 /mL VBB-*S. aureus*; c: 0.65×10^5 /mL VBB-*S. aureus*; d: 1.3×10^5 /mL VBB-*S. aureus*; e: 2.6×10^5 /mL VBB-*S. aureus*; f: 5.2×10^5 /mL VBB-*S. aureus*; g: 7.8×10^5 /mL VBB-*S. aureus*; h: 10.4×10^5 /mL VBB-*S. aureus*.

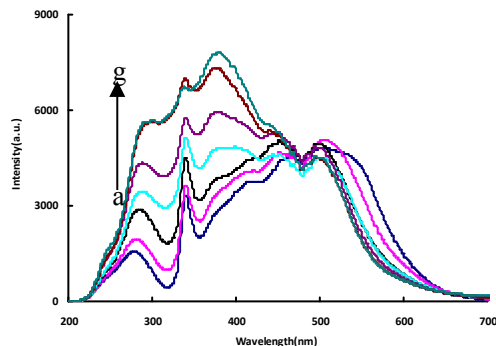
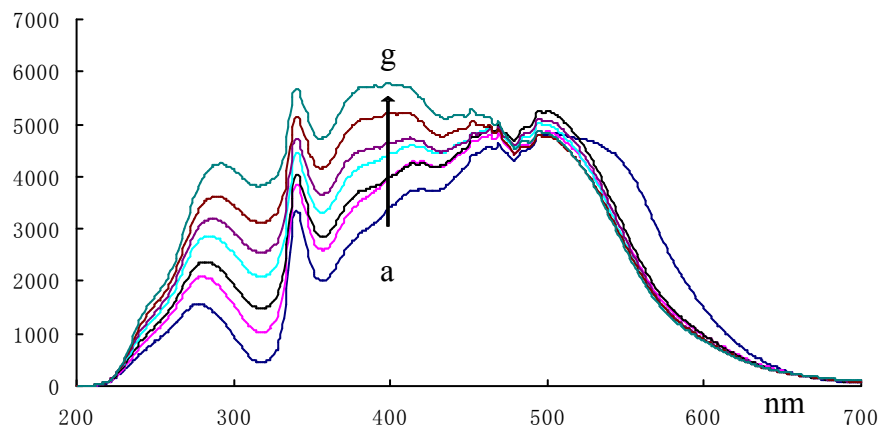


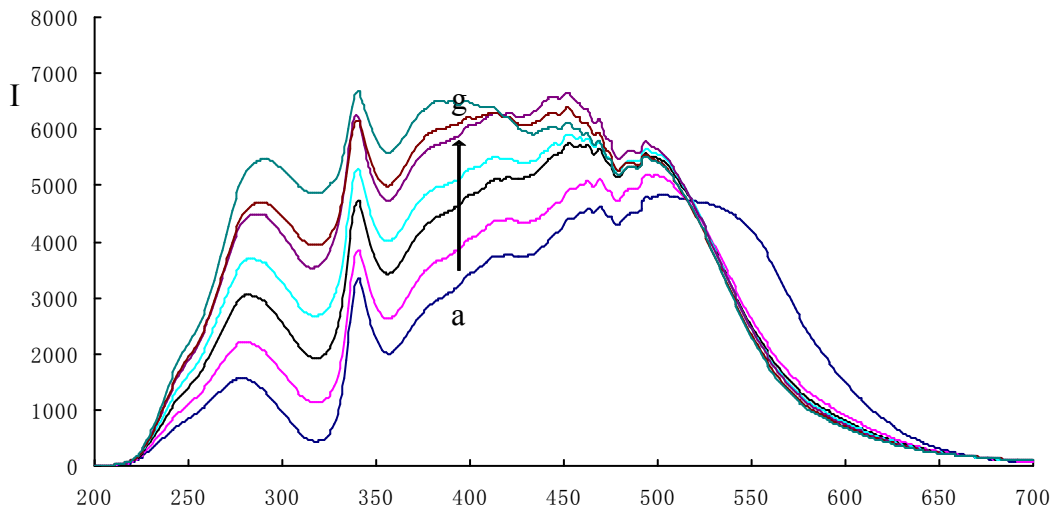
Fig.S13 RRS spectra of AgNPs-NaCl-VBB-*E. coli*. a: 5 μ g/mL AgNRs- 1.5×10^{-3} mol/L NaCl-0.01 μ g/mL AgNO₃-pH 6.8 PBS; b: a+ 1.0×10^8 cfu/mL VBB-*E. coli*; c: a+ 2.0×10^8 cfu/mL VBB-*E. coli*; d: a+ 4.0×10^8 cfu/mL VBB-*E. coli*; e: a+ 8.0×10^8 cfu/mL VBB-*E. coli*; f: a+ 12×10^8 cfu/mL VBB-*E. coli*; g: a+ 16×10^8 cfu/mL VBB-*E. coli*.



Wavelength/nm

Fig. S14 RRS spectra of AgNPs-NaCl-AgNO₃-VBB- *S. aureus*

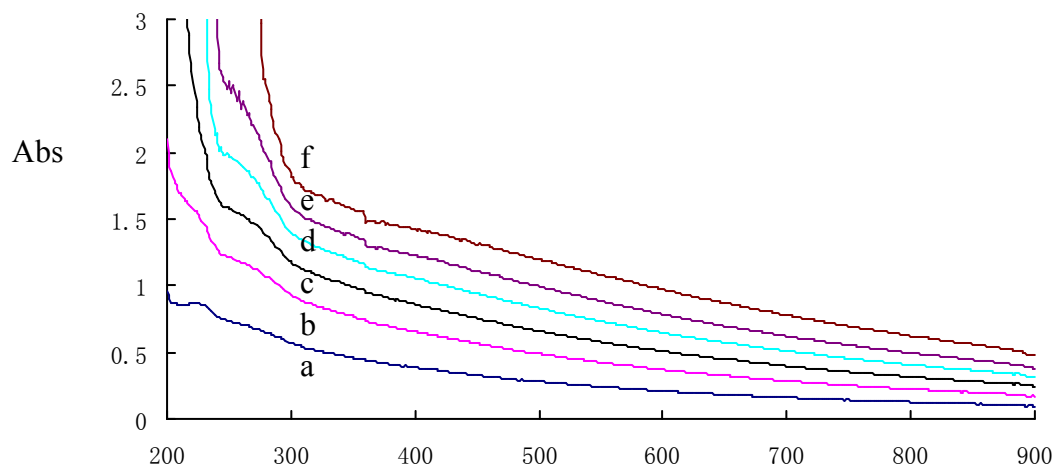
a: 5 µg/mL AgNPs -1.5×10⁻³ mol/L NaCl-0.01 µg/mL AgNO₃-pH 6.8 PBS; b: a- 1.6×10⁵/mL VBB-*S. aureus*; c: a- 3.2×10⁵/mL VBB-*S. aureus*; d: a- 4.8×10⁵/mL VBB-*S. aureus*; e: a-6.4×10⁵/mL VBB-*S. aureus*; f: a- 8.0×10⁵/mL VBB-*S. aureus*; g: a- 9.6×10⁵/mL VBB-*S. aureus*.



Wavelength/nm

Fig. S15 RRS spectra of AgNPs-NaCl-VBB- *B. subtilis*

a: 5 µg/mL AgNPs -1.5×10⁻³ mol/L NaCl-0.01 µg/mL AgNO₃-pH 6.8 PBS; b: a- 1.25×10⁸/mL *B. subtilis*; c: a- 2.5×10⁸/mL *B. subtilis*; d: a- 3.75×10⁸/mL *B. subtilis*; e: a- 5.0×10⁸/mL *B. subtilis*; f: a- 6.25×10⁸/mL *B. subtilis*; g: a- 7.5×10⁸/mL *B. subtilis*.



Wavelength/nm

Fig. S16 Absorption spectra *E. coli*

a: 1.5×10⁹/mL *E. coli*; b: 3.0×10⁹/mL *E. coli*; c: 4.5×10⁹/mL *E. coli*; d: 6.0×10⁹/mL *E. coli*; e: 7.5×10⁹/mL *E. coli*; f: 9.0×10⁹/mL *E. coli*.

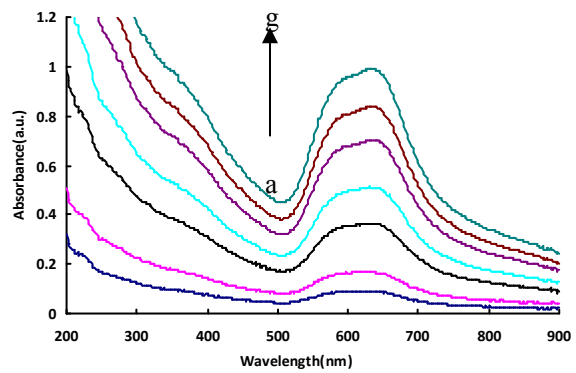


Fig. S17 Absorption spectra of VBB- *E. coli*. a: 0.6×10^9 cfu/mL VBB-*E. coli*; b: 1.2×10^9 cfu/mL VBB-*E. coli*; c: 2.4×10^9 cfu/mL VBB-*E. coli*; d: 3.6×10^9 cfu/mL VBB-*E. coli*; e: 4.8×10^9 cfu/mL VBB-*E. coli*; f: 6.0×10^9 cfu/mL VBB-*E. coli*; g: 7.2×10^9 cfu/mL VBB-*E. coli*.

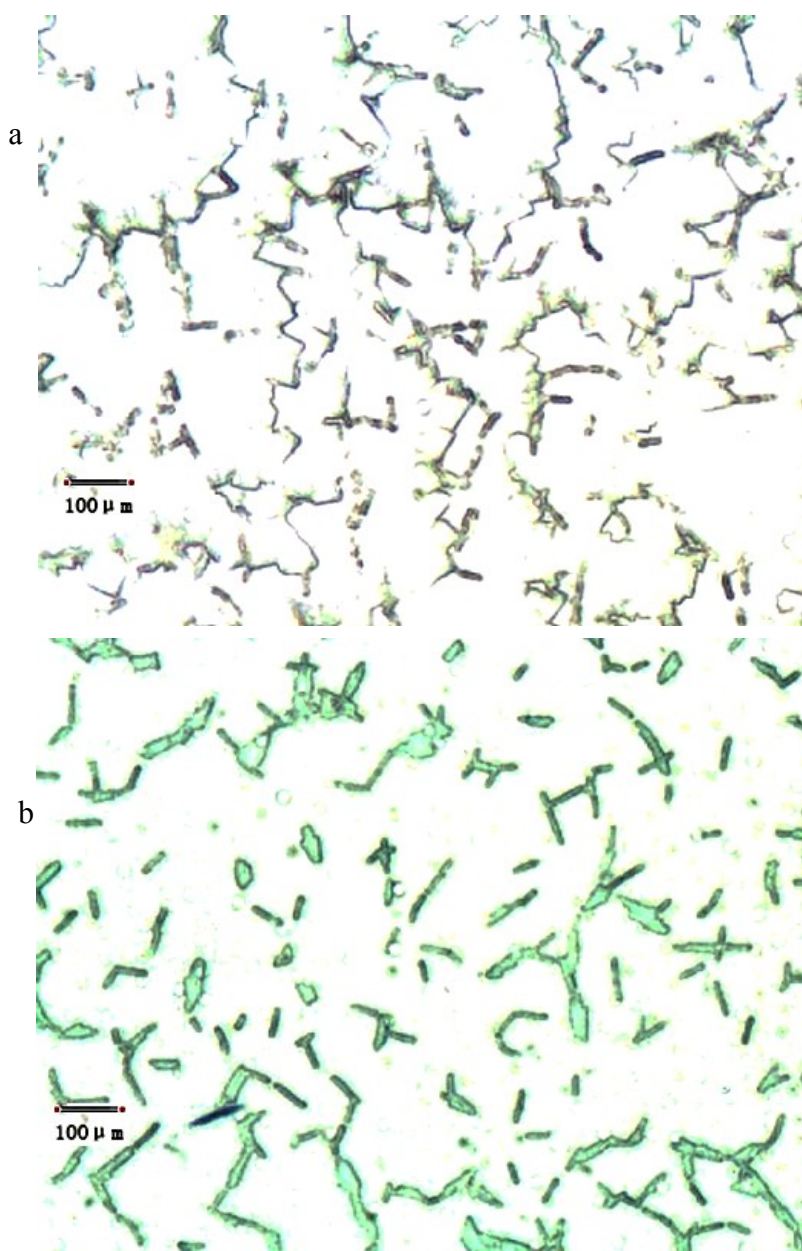


Fig. S18 Optical micrographs of *E. coli*

a: *E. coli*; b: VBB-*E. coli*

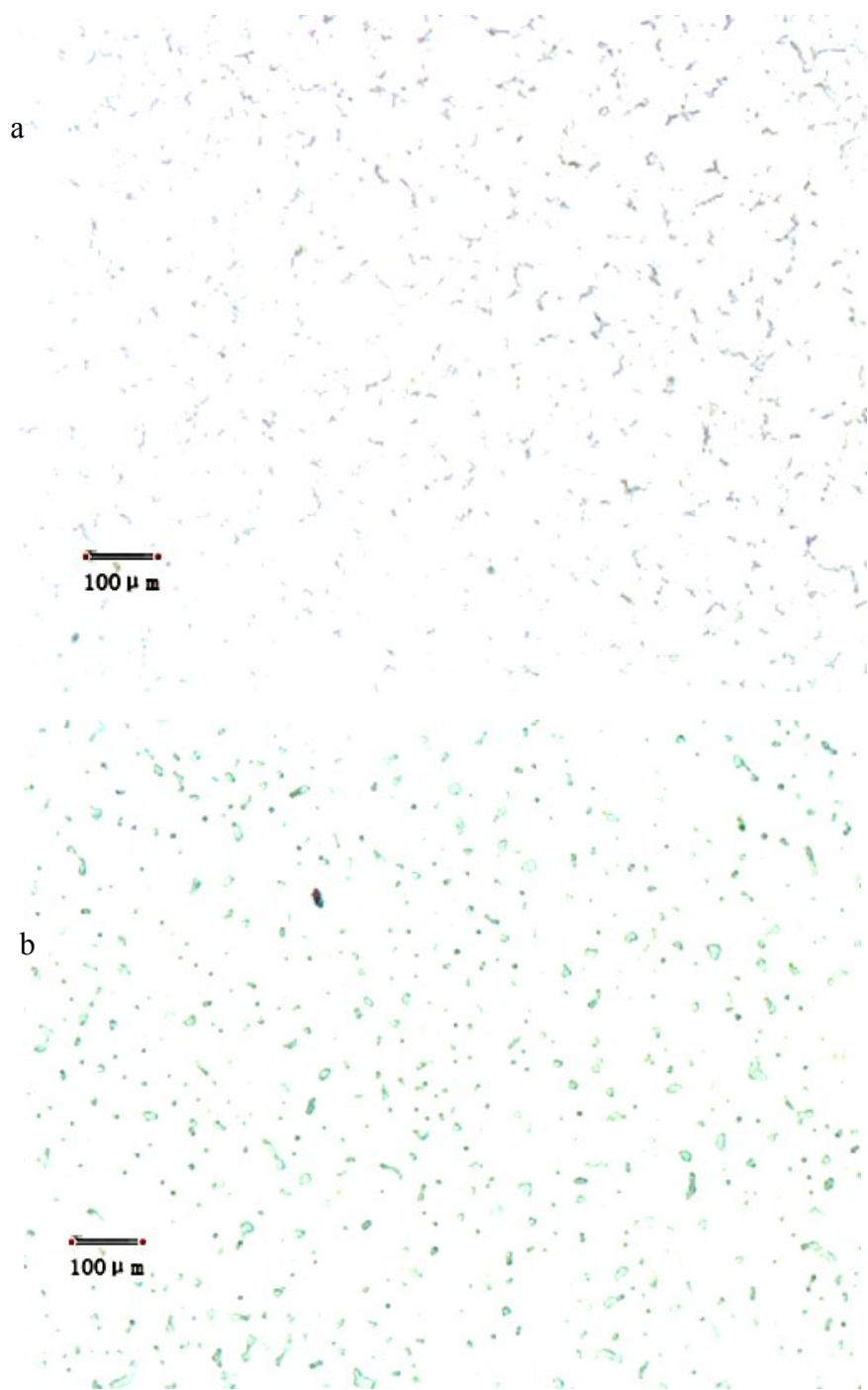


Fig. S19 Optical micrographs of aureus

a: *S. aureus*; b:VBB-*S. aureus*



Fig. S20 Optical micrographs of *subtilis*

a: *B. subtilis*; b: VBB-*B. subtilis*

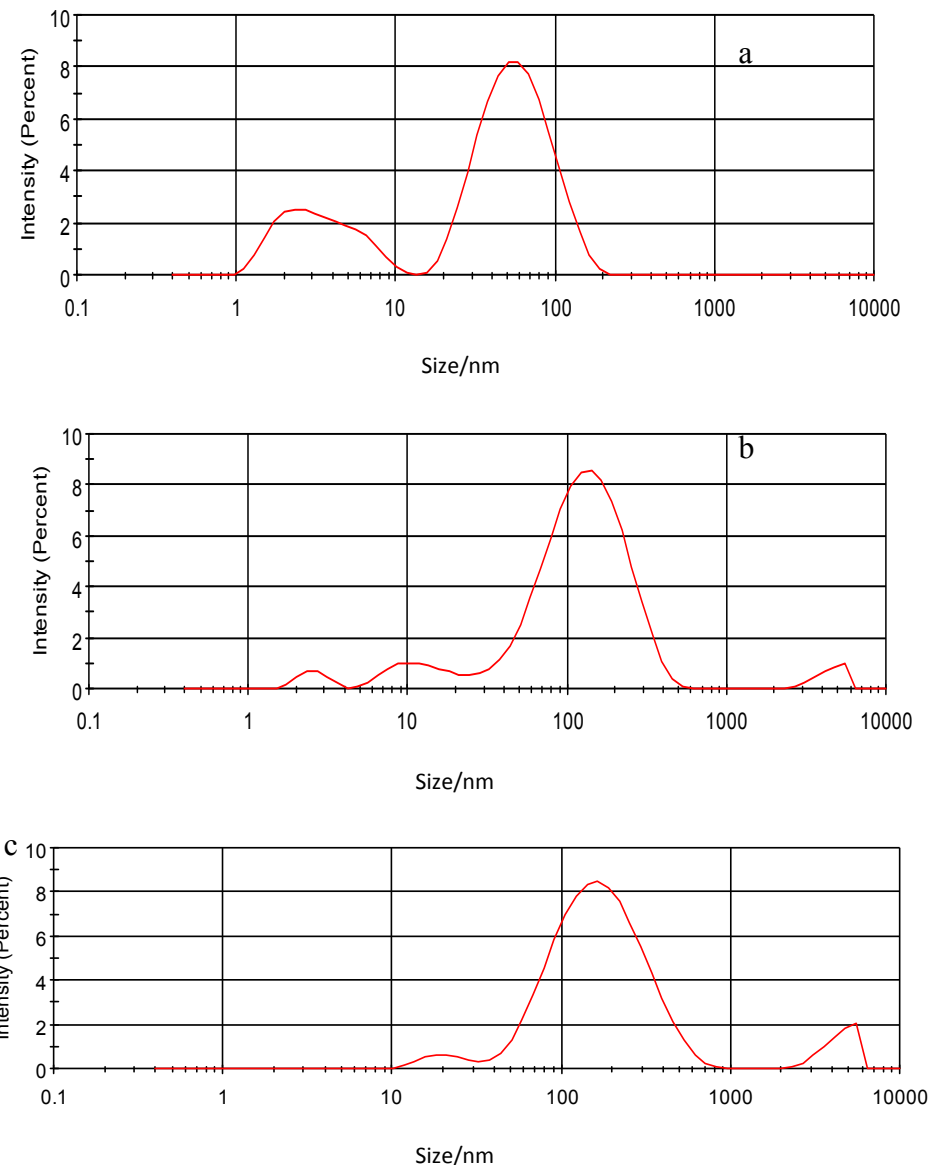
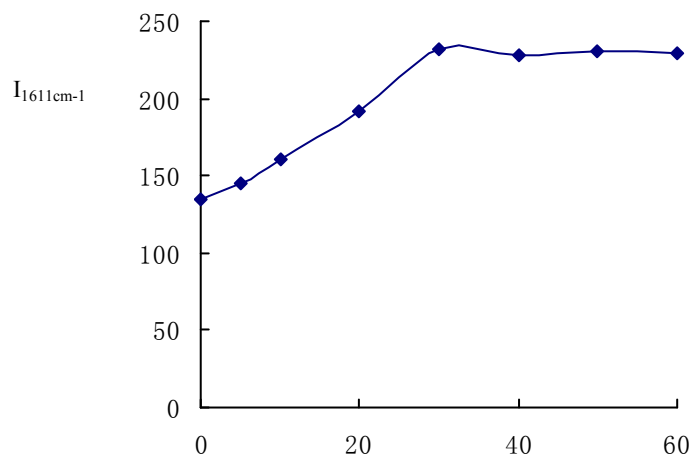


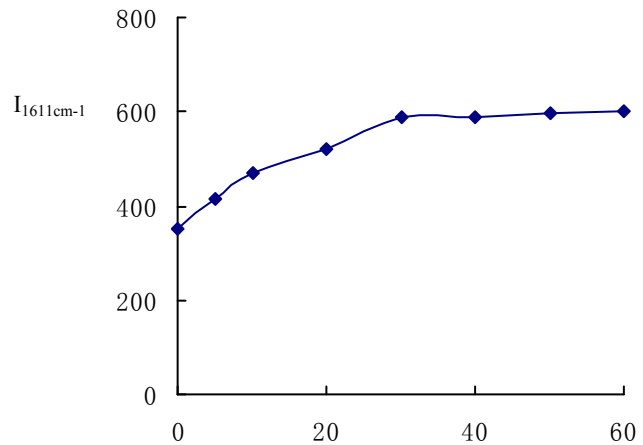
Fig. S21 Laser scattering diagram of AgNPs-NaCl-AgNO₃-VBB-*E. coli*

a: 5 µg/mL AgNPs-1.5×10⁻³ mol/L NaCl -1 µmol/mL AgNO₃-pH 6.8 PBS; b:a 7.5×10⁸/mL VBB-*E. coli*; c:a-3×10⁹/mL VBB-*E. coli*.



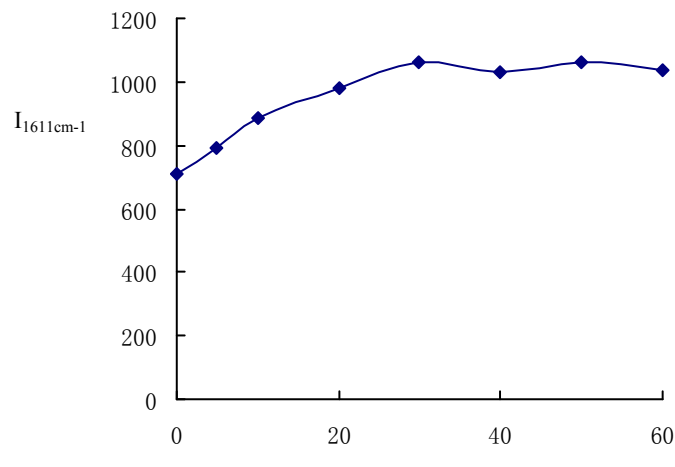
time/min

Fig. S22 Effect of staining time in staining process (*E. coli*)



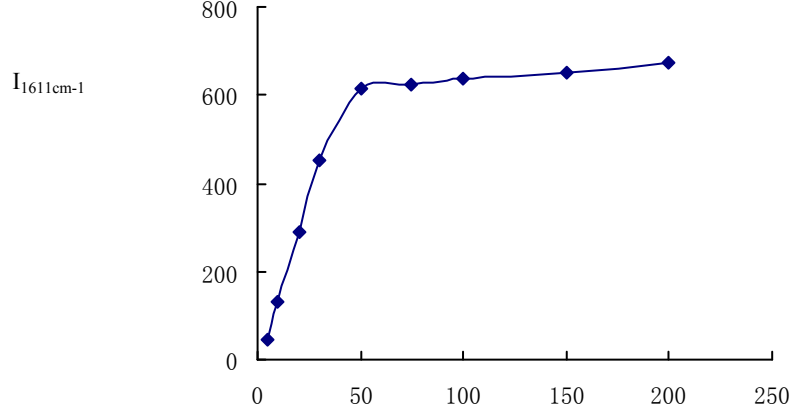
time/min

Fig. S23 Effect of staining time in staining process (*S. aureus*)



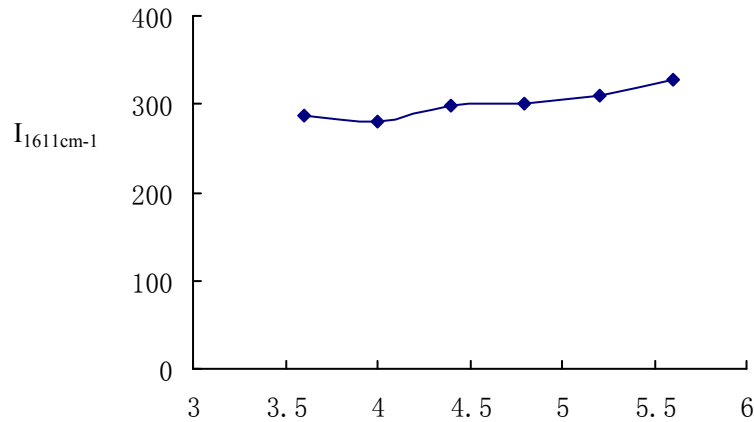
time/min

Fig. S24 Effect of staining time in staining process (*B. subtilis*)



$\mu\text{mol/L}$

Fig. S25 Effect of VBB concentration in staining process



pH

Fig. S26 Effect of pH NaAc-HAc buffer solution in staining process

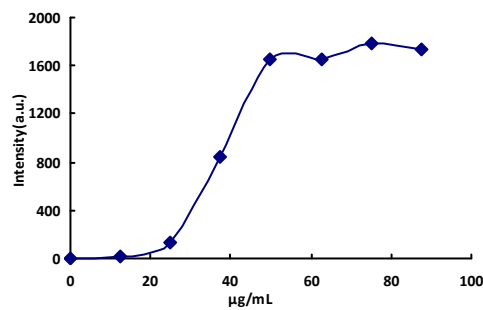
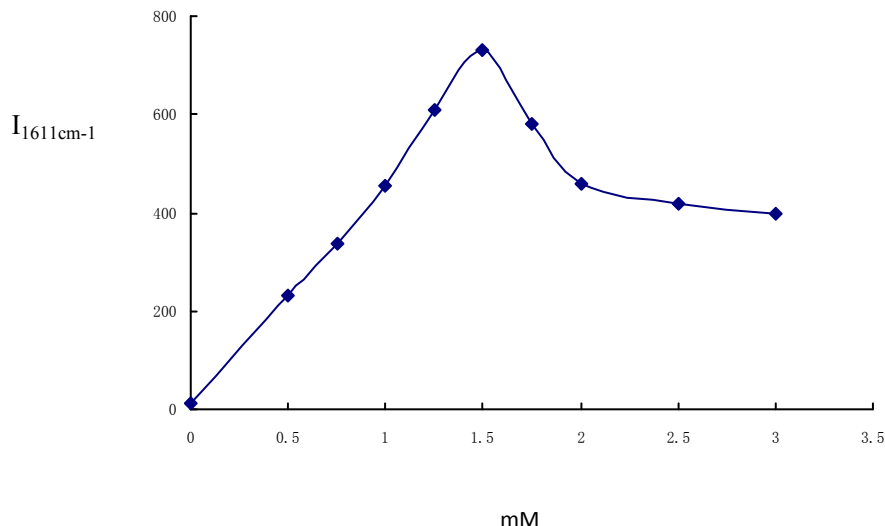


Fig.S27 Effect of AgNPs concentration in detecting process



mM

Fig. S28 Effect of NaCl concentration in detecting process

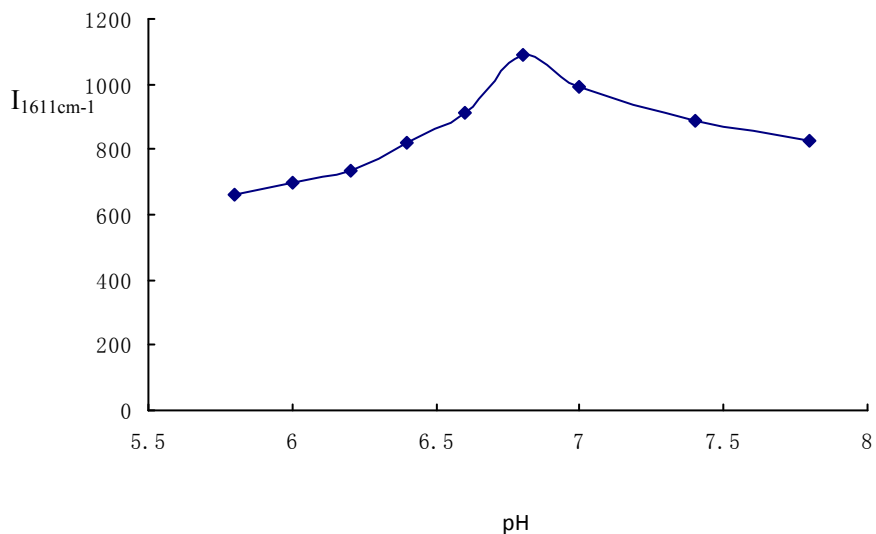


Fig. S29 Effect of pH PBS buffer solution in detecting process

Table S1 Stability of AgNRs

Intensity \ Days	1	2	3	5	7	10	13	18	23	28	33	38
$A_{444\text{nm}}$	0.192	0.189	0.197	0.184	0.185	0.200	0.195	0.187	0.199	0.210	0.229	0.236
$I_{1611\text{cm}^{-1}}$	2520	2666	2519	2681	2395	2473	2510	2600	2629	2467	2903	1936

Table S2 Assignment of SERS peaks different for molecular probes in AgNPs sol

Molecular probes	Peak positions/intensity	Vibration mode	Structure
VBB	198 m	Skeletal bending	
	432 w	$\nu(C=N), \nu(C=C)$	
	677 w	$\gamma(CH)$	
	793 m	$\gamma(C-C)$	
		Aromatics	
		$\nu(C-C)$	
	1165 s	Aromatics, $\delta(CH)$	
	1199 s	$\delta(CH), \delta(CH_3)$	
	1364 s	$\nu(C-N), \delta(CH_3)$	
	1392 vs	$\nu(circle), \nu(C-N)$	
VB4R	1445 m	$\delta(CH_3)$	
	1478 m	$\delta(circle)$	
	1562 m	$\delta(CH)$	
	1611 vs	$\nu(C=N), \nu(N-H)$	
	214 m	Skeletal bending	
	431 w	$\delta(CH)$	
	676 w	$\gamma(CH)$	
	797 m	$\gamma(C-C)$	
		Aromatics	
	1167 s	$\nu(C-C)$	
ST	1167 s	Aromatics, $\delta(CH)$	
	1200 s	$\delta(CH), \delta(CH_3)$	
	1374 s	$\nu(C-N), \delta(CH_3)$	
	1385 vs	CH in $\delta(CH)(C=C)$	
	1444 m	$\delta(CH_3)$	
	1565 s	$\nu(C=N), \nu(N-H)$	
	1611 vs	$\nu(C=N), \nu(C=C)$	
	188 w	Skeletal bending	
	431 s	$\delta(CH)$	
	679 m	$\gamma(CH)$	
AR	795 s	$\gamma(C-C)$	
		Aromatics	
	1167 s	$\nu(C-C)$	
		Aromatics, $\delta(CH)$	
	1200 s	$\delta(CH), \delta(CH_3)$	
	1366 s	$\nu(C-N), \delta(CH_3)$	
	1391 vs	CH in $\delta(CH)(C=C)$	
	1613 vs	$\nu(C=N), \nu(C=C)$	
	205 m	Skeletal bending	
	492 m	$\gamma(CH) \sigma(C-Cl)$	
AR	749 m	$\nu(circle)$	
		$\delta(CH_2)$	
	1321 s	Aromatics	
	1368 vs	$\nu(C-C)$ Aromatics	
	1484 m	$\delta(NH)$	
	1642 m	$\nu(C-C)$ Aromatics	

σ : stretching vibration; δ : bending vibration; δs : symmetric bending vibration; $\nu(\text{circle})$: ring breathing; $\delta(\text{circle})$: inner surface deformation of the ring; $\gamma(\text{CH})$: outside surface deformation of CH; $\gamma(\text{circle})$: outer surface deformation; ρ —rocking, in plane bending; γ —wagging

Raman Intensity: vs: very strong; s: strong; m: medium; w: weak.

Table S3 SERS intensity of VBB and VBB-*E. coli* molecular probe

Raman shift (cm ⁻¹)	Intensity (VBB)	SERS intensity ratio of the I _{1611 cm⁻¹}	Intensity (VBB- sbacteria)	SERS intensity ratio of the I _{1611 cm⁻¹}
198	370	0.40	429	0.44
432	349	0.38	354	0.36
677	261	0.28	376	0.38
793	316	0.34	558	0.57
1165	481	0.52	876	0.89
1199	454	0.49	834	0.85
1364	487	0.53	800	0.81
1392	652	0.71	936	0.95
1611	920	1.00	983	1.00

Table S4 SERS intensity of dyes

Dyes	Max intensity (cm ⁻¹)	Dyes	Max intensity (cm ⁻¹)
VBB	1084 (1611)	Crystal violet	328 (796)
VB4R	989 (1611)	Orange II	40 (1390)
SafranineT	276 (1613)	Rhodamine B	60 (616)
Peafowl green	68 (612)	Indigo blue	57 (1619)
Basic orange	50 (1379)	Acridine red	197 (1368)

Table S5 SERS effect comparison of different silver nanoparticles

Silver nanoparticles*	Sensitizer	Probe	I _{1611 cm⁻¹}
Spherical	NaCl, AgNO ₃	VBB	441
Triangle	NaCl, AgNO ₃	VBB	756
AgNPs	NaCl, AgNO ₃	VBB	1149
AgNPs/0.001% GO	NaCl, AgNO ₃	VBB	757
AgNPs/0.002% GO	AgNO ₃	VBB	365

The Ag concentration of nanoparticles was 5 μg/mL, NaCl: 1.5×10⁻³ mol/L, AgNO₃: 0.01 μg/mL, VBB: 1.0×10⁻⁶ mol/L

Table S6 Effect of foreign substances in detecting progress (5.0×10^8 cfu/mL *E. coli*)

Coexistent substance	Tolerance concentration	Relative error (%)	Coexistent substance	Tolerance concentration	Relative error (%)
Ca ²⁺	0.8 mmol/L	5.0	Br ⁻	0.8 mmol/L	4.0
Zn ²⁺	0.5 mmol/L	3.3	F ⁻	1.0 mmol/L	6.2
Mg ²⁺	0.6 mmol/L	-4.0	NO ₃ ⁻	0.4 mmol/L	-5.0
Ba ²⁺	0.4 mmol/L	-5.0	ClO ₄ ⁻	0.6 mmol/L	4.5
Cu ²⁺	0.3 mmol/L	4.6	CO ₃ ²⁻	0.5 mmol/L	5.6
Co ²⁺	0.7 mmol/L	3.0	SO ₄ ²⁻	0.8 mmol/L	-2.8
<i>B. subtilis</i>	5.0×10^7 cfu/mL	9.0	<i>S. aureus</i>	1.5×10^9 cfu/mL	9.0

Table S7 Analytical characteristic of detecting *B. subtilis*

Methods	System	LR(cfu/mL)	Regress equation	R ²	DL(cfu/mL)
SERS	AgNPs-NaCl-VBB- <i>B. subtilis</i>	3×10^6 - 2×10^9	$\Delta I_{1611} = 206.5c + 18.5$	0.9982	1×10^6
	Unstained <i>B. subtilis</i>	5×10^6 - 6×10^9	$\Delta I_{295} = 266.4c + 311.6$	0.9968	2×10^6
RRS	VBB- <i>B. subtilis</i>	6×10^6 - 5×10^9	$\Delta I_{295} = 193.4c + 286.8$	0.9942	2×10^6
	AgNPs-NaCl- VBB- <i>B. subtilis</i>	6×10^6 - 1.5×10^9	$\Delta I_{340} = 550.6c + 107.8$	0.9879	2×10^6

Table S8 Analytical characteristic of detecting *S. aureus*

Methods	System	LR(cfu/mL)	Regress equation	R ²	DL(cfu/mL)
SERS	AgNPs-VBB- <i>S. aureus</i>	1×10^3 - 2×10^6 cfu/mL	$\Delta I_{1611} = 62.5c + 5.0$	0.9998	1×10^3 cfu/mL
	Unstained <i>S. aureus</i>	3×10^3 - 3×10^6 cfu/mL	$\Delta I_{295} = 34.8c + 312.6$	0.9957	2×10^3 cfu/mL
RRS	VBB- <i>S. aureus</i>	2×10^3 - 2×10^6 cfu/mL	$\Delta I_{295} = 54.2c + 117.4$	0.9975	2×10^6 cfu/mL
	AgNPs- VBB- <i>S. aureus</i>	3×10^3 - 4×10^6 cfu/mL	$\Delta I_{340} = 28.9c + 37.1$	0.9955	2×10^6 cfu/mL

Table S9 Comparison of different analytical methods for the detection of bacteria

Methods	Principle	Liner range cfu/mL	DL	Comment	Refs
PCR	Utilized multiplex PCR		2×10 ⁴ cfu/mL	Classic, but long process	24
ELISA	An indirect ELISA method was used to detect the presence of pathogenic bacteria in vegetables		10 ³ cfu/g	Good selectivity, but complex procedure	25
Nucleic acid aptamer analysis	Obtained a panel of ssDNA aptamers specific against <i>S. aureus</i> by the subtractive SELEX, and demonstrated a superior effect of the combined use of these aptamers compared to an individual aptamer in the recognition of different strains of <i>S. aureus</i> or cells in different growth states.			Good selectivity, but complex procedure.	26
Voltammetry	Aureus aptamer was immobilized on streptavidin coated magnetic beads (MB), which serves as a capture probe. A secondary anti- <i>S. aureus</i> aptamer was conjugated to silver nanoparticles that sensitively reports the detection of the target. In the presence of target bacterium, an Apt/S.aureus/apt-AgNP sandwich complex is formed on the MB surface and the electrochemical signal of AgNPs followed through anodic stripping voltammetry.	10 - 1×10 ⁶ cfu/mL	1 cfu/mL	Sensitivity, but complex procedure.	27
Biosensor	Rapid detection and quantification of <i>E. coli</i> O157:H7 in meat and water samples based on the electrocatalytic properties of AuNP towards hydrogen evolution reaction and superparamagnetic microbeads as pre-concentration/purification platforms without the need of broth enrichment is developed for the first time.	100 - 1×10 ⁵ cfu/mL	309 cfu/mL	Sensitivity, but complex principle.	28
VBB-bacteria SERS	In the AgNPs substrate, VBB-bacteria have a strong SERS peak at 1611 cm ⁻¹ . The SERS signal is increased with the increased concentration of VBB-bacteria in a certain range.	10-700 cfu/mL	10 cfu/mL	Sensitive, simple, and rapid.	This method

Table S10 VBB-bacteria SERS intensity of different culture time

T	c(<i>E.coli</i>)	0	10	50	100	300	500	700
6h	-	-	-	-	-	-	-	-
9h	-	-	-	-	-	-	-	199
12h	-	107	244	323	644	982	1123	